

YALE PEABODY MUSEUM

P.O. BOX 208118 | NEW HAVEN CT 06520-8118 USA | PEABODY.YALE. EDU

JOURNAL OF MARINE RESEARCH

The *Journal of Marine Research*, one of the oldest journals in American marine science, published important peer-reviewed original research on a broad array of topics in physical, biological, and chemical oceanography vital to the academic oceanographic community in the long and rich tradition of the Sears Foundation for Marine Research at Yale University.

An archive of all issues from 1937 to 2021 (Volume 1–79) are available through EliScholar, a digital platform for scholarly publishing provided by Yale University Library at <https://elischolar.library.yale.edu/>.

Requests for permission to clear rights for use of this content should be directed to the authors, their estates, or other representatives. The *Journal of Marine Research* has no contact information beyond the affiliations listed in the published articles. We ask that you provide attribution to the *Journal of Marine Research*.

Yale University provides access to these materials for educational and research purposes only. Copyright or other proprietary rights to content contained in this document may be held by individuals or entities other than, or in addition to, Yale University. You are solely responsible for determining the ownership of the copyright, and for obtaining permission for your intended use. Yale University makes no warranty that your distribution, reproduction, or other use of these materials will not infringe the rights of third parties.



This work is licensed under a Creative Commons Attribution-NonCommercial-ShareAlike 4.0 International License.
<https://creativecommons.org/licenses/by-nc-sa/4.0/>



Dynamics of the Makassar Strait

by Jorina M. Waworuntu^{1,2}, Silvia L. Garzoli³ and Donald B. Olson¹

ABSTRACT

Data collected as part of the Arlindo Project (“Arlindo” is an acronym for Arus Lintas Indonesia, meaning “throughflow” in Bahasa Indonesia) from October 1996 to March 1998 are analyzed to study the characteristics of the flow through the Makassar Strait. Analysis of inverted echo sounders (IES) and bottom pressure data (PIES) combined with TOPEX/POSEIDON satellite-derived sea height anomaly suggest that a minimum of three-layer approximation is necessary to explain the dynamics of the flow in the Makassar Strait. The simple two-layer model used in several studies of the throughflow is rejected based on total incompatibility with the data sets. A three-layer model with significant contributions by the middle layer provides a consistent interpretation of PIES and satellite data. Results are interpreted in the framework of the large-scale circulation.

1. Introduction

The primary goal of the Indonesia-United States Arus Lintas Indonesia (Arlindo) or throughflow project is to study the circulation and water mass stratification within the Indonesian Seas in order to formulate a thorough description of the source, spreading patterns, inter-ocean transport and dominant mixing processes. As part of this project, a small array of inverted echo sounders, equipped with pressure gauges (PIES), were deployed along the main axis of the Makassar Strait (Fig. 1). The objective of these PIES was to measure the meridional throughflow by monitoring the pressure gradient along the Strait. Results from PIES measurements will be compared to current meter observations in order to see if PIES might be used to monitor the throughflow effectively, rather than the much more operationally difficult, direct velocity measurements. The Makassar Strait is observed to be the main conduit of water through the Indonesian Seas (Field and Gordon, 1992; Bingham and Lukas, 1995; Ilahude and Gordon, 1996; Gordon and Fine, 1996; Hautala *et al.*, 1996; Gordon *et al.*, 1998; Gordon and Susanto, 1999; Waworuntu *et al.*, 1999). In this paper only the low-frequency analysis of the data will be presented.

Inverted echo sounders (IES) are bottom-deployed instruments that measure the time that it takes an acoustic signal to travel from the bottom to the surface and back (travel

1. Rosenstiel School of Marine and Atmospheric Science, University of Miami, Miami, Florida, 33149, U.S.A.

2. Present address: Environment Department, PT Newmont Nusa Tenggara, Jalan Pendidikan 64, Mataram 83125, Indonesia. *email*: jwaw4296@corp.newmont.com

3. National Ocean and Atmospheric Administration, Atlantic Oceanographic and Meteorological Laboratory, 4301 Rickenbacker Causeway, Miami, Florida, 33149, U.S.A.

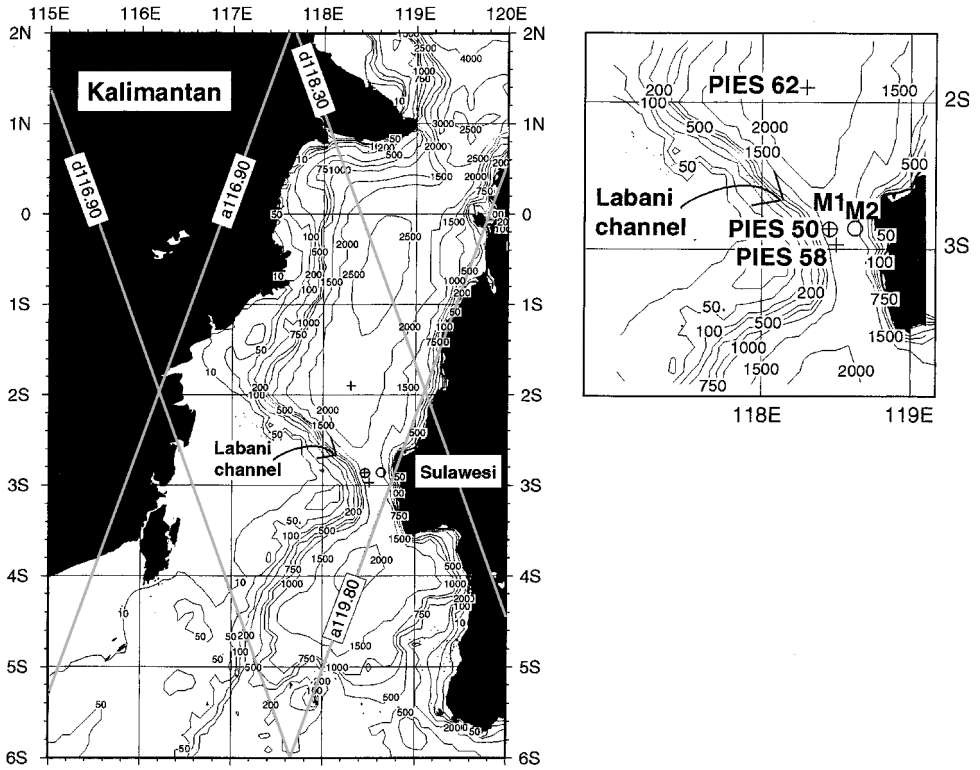


Figure 1. Location of the Makassar PIES array (crosses) and current meters M1 and M2 (circles). Superimposed are the T/P ground tracks in gray.

time). In general this travel time, τ , has proved to be directly related to the depth of the thermocline (Watts and Rossby, 1977). It can also be related to dynamic height (Garzoli and Garraffo, 1989; Garzoli, 1993). IES were successfully used to monitor the zonal pressure gradient along the equatorial Atlantic (Katz, 1977). They have been combined with hydrographic and satellite altimetry to provide detailed descriptions of the Gulf Stream (Kelly and Watts, 1994), and the southeastern Atlantic dynamics (Garzoli *et al.*, 1997).

Four PIES were deployed from the Indonesian research ship, *Baruna Jaya IV*, in November 1996. The instruments were recovered in February 1999. Unfortunately only three of the four PIES were recovered (PIES 50 at 2.86S 118.45E, PIES 58 at 2.97S 118.50E, and PIES 62 at 1.90S 118.30E), and PIES 62 had a shorter record. PIES 50 and 58 were deployed at 2138 m depth and 2147 m depth and PIES 62 at 2228 m depth. Data at sites 58 and 50 are redundant. Only data from PIES 50 and PIES 62 are used in the present analysis.

During the deployment cruise, Acoustic Doppler Current Profiler (ADCP) measurements were collected twice along a line 3 nm to the west of the PIES, which passed through the current meter mooring (CMM) M1 location (Gordon and Susanto, 1999). Conductivity-

Temperature-Depth (CTD) stations were obtained at the site of deployments for further calibration of the PIES time series. During the recovery cruise, additional hydrographic data were collected as well as direct measurements of the surface currents using ADCP.

2. Data reduction and calibration

The 15-month-long travel time and bottom pressure series collected with the PIES were reduced using standard procedures. After the series were despiked and missing points interpolated, the travel time series were scaled to physical parameters. Using CTD profiles from four Arlindo cruises (August 1993 (AM93), February 1994 (AM94), November 1996 (AC96), and February 1998 (AC98)) the relationships between travel time and the dynamic height, the integrated temperature, and the depth of the thermocline, in the Makassar Strait region were studied (Fig. 2). The travel time, τ , is highly correlated to the integrated temperature. The squared correlation coefficient, R^2 , between integrated temperature and τ from surface to 1500 m is equal to 0.97, with an error on the estimate of $\pm 0.030^\circ\text{C}$. On the other hand, the regression between changes in dynamic height (from surface relative to dynamic height at 1500 m) to τ gives a rather low R^2 of 0.69 and a large error of ± 0.049 dynm. This is due to the presence of very low salinity water at the surface layer in the Makassar Strait during AM94 and AC96 that led to an increase in dynamic height during that period. If we exclude the upper layer and use dynamic height of 150 m relative to 1500 m, R^2 increases to 0.925 and the error reduced to ± 0.007 dynm. Very weak correlation exists between the depth of the 15°C isotherm and τ . The correlation coefficient, $R^2 = 0.321$, corresponds to an error in the estimate of the isotherm of ± 10 m. The 15°C isotherm is chosen because it represents the main thermocline in that it falls near the maximum in instability at the bottom of the subtropical waters (Ilahude and Gordon, 1996).

The bottom pressure series, p_b , were linearly de-trended to eliminate any possible drift in the sensors. The pressure sensor drift for PIES 50 is equal to 0.089 bar/year and for PIES 62 is equal to 0.031, much larger than the pressure variability that is in the order of ± 0.01 bar. Bottom-deployed pressure sensors provide a measurement of the variability in barotropic pressure. Using ADCP data and the current meter series, the variability in p_b can be scaled to velocity (Garzoli *et al.*, 1996). The time series of the data collected at sites PIES 50 and PIES 62 are shown in (Fig. 3). The series has been demeaned and filtered to eliminate the tidal signal that is dominant in p_b and strong in the τ series. The increase in τ during the measurement period (Fig. 3a) is correlated to the decrease in the integrated temperature in the water column. In December 1996 and the beginning of January 1997, τ decreases for about one month. A sharp increase in τ is observed in July 1997.

The bottom temperature series (Fig. 3b) show warm events of a $0.03\text{--}0.05^\circ\text{C}$ that are significantly above the background oscillating temperature of $\pm 0.01^\circ\text{C}$ around the mean. These warm events are observed only at PIES 50 and PIES 58 located at the constriction point. These warm events coincide with northward-flowing current, measured by the deepest current meter MAK1, at 1500 m (Fig. 4). The northward-flowing current at 1500 m

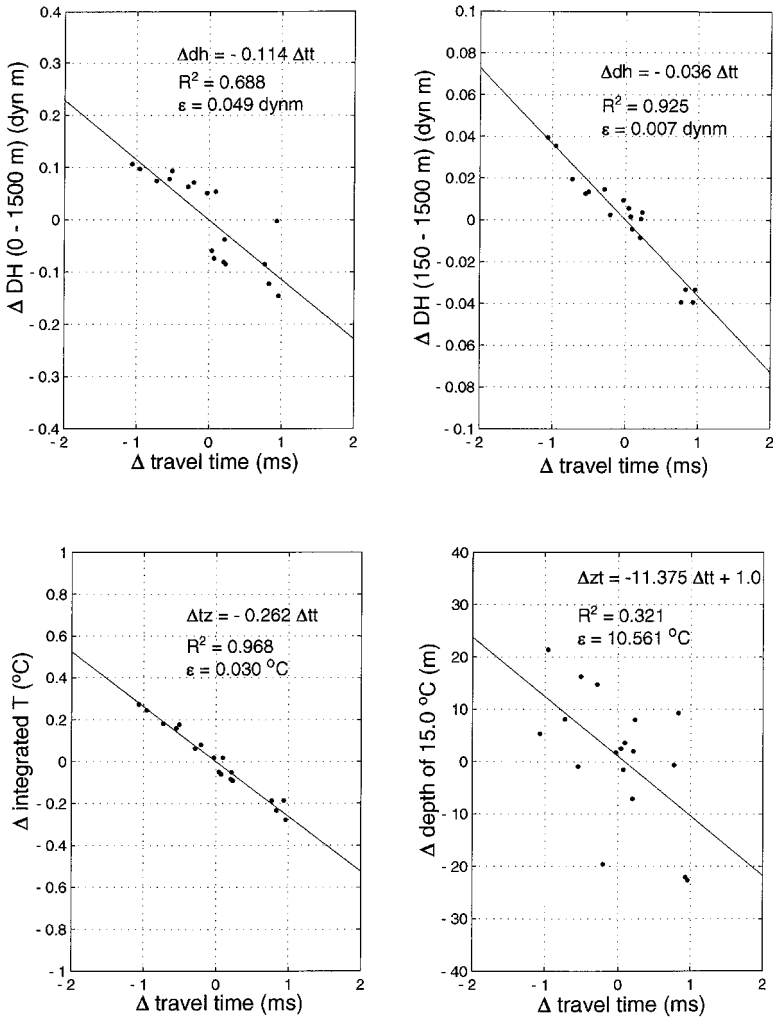


Figure 2. Correlation between τ and dynamic height, integrated temperature, and depth of the thermocline, in the Makassar Strait.

is 180° out of phase with the current at 700 m (Gordon *et al.*, 1998). Whenever there was a strong southward flow at the intermediate level, the 600 m sill at the southern end of the Makassar Strait blocks the flow and pushed the isotherms down, resulting in a northward warm flow at the bottom layer. The PIES 62 record (located north of the constriction) shows no warm events. At the PIES 62 location, the bottom temperature is almost constant, varying only by about $\pm 0.007^{\circ}$ C.

From the deployment in November 1996 until mid February 1997, p_b increased (Fig. 3c). Afterward, the trend switched and p_b decreased until the end of the record. A slight increase in p_b is observed in July 1997.

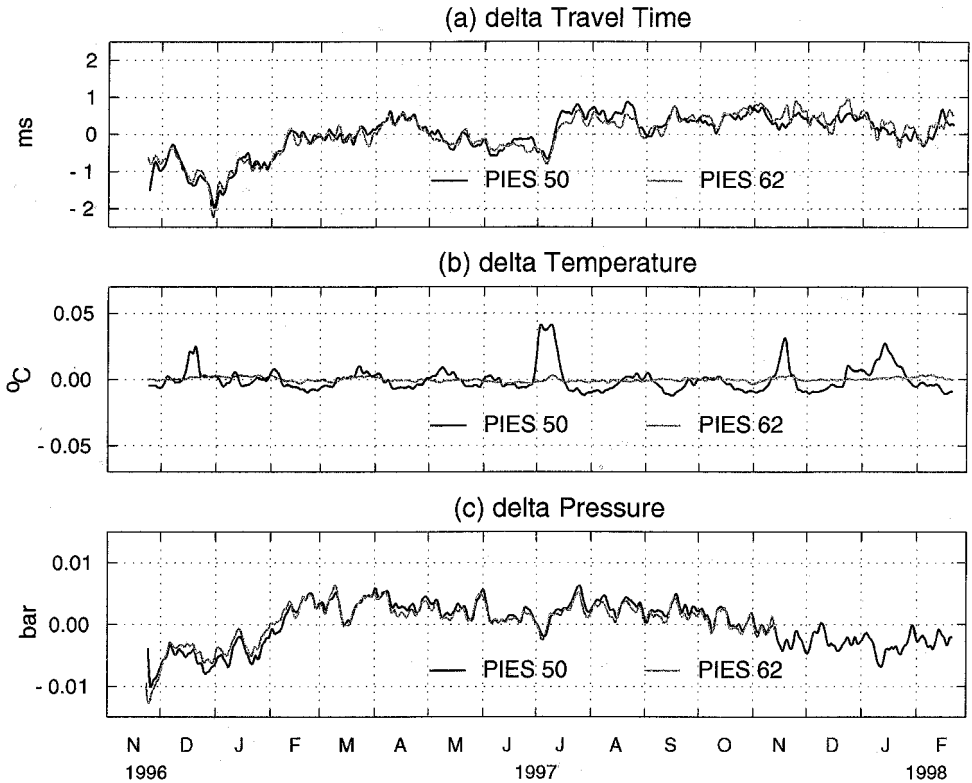


Figure 3. Variability of travel time (a), bottom temperature (b), and bottom pressure (c) measured by PIES 62 and PIES 50.

3. Data analysis and interpretation

a. Barotropic transport

In a narrow channel, in which the effects of rotation can be neglected, the mean flow is directed in the direction along the channel. In order for the effects of rotation to be negligible the width of the channel, W , must be small compared with the Rossby radius of deformation (R_r) or $W/R_r \ll 1$. For barotropic flow, $R_r = (gH)^{1/2}/|f|$. At latitude 3.5S the Makassar Strait has a width $W = 44000$ m, $H = 2100$ m, $f = -8.903 \times 10^{-6} \text{ s}^{-1}$, $g = 9.8 \text{ ms}^{-1}$, $R_r = 16 \times 10^6$ m resulting in $W/R_r = 0.003 \ll 1$. For baroclinic flow, the internal Rossby radius of deformation $R_i = (g'h_1)^{1/2}$, where g' is the reduced gravity and h_1 is the depth of the upper layer. For $g' = 0.03 \text{ ms}^{-1}$ and $h_1 = 100$ m, $R_i = 227 \text{ km} \gg W$.

The Bernoulli equation governs the motion in a narrow channel:

$$\left(\frac{V_N^2}{2} + gz_N + \frac{p_{bN}}{\rho_0} \right) - \left(\frac{V_S^2}{2} + gz_S + \frac{p_{bS}}{\rho_0} \right) = \lambda \frac{l}{d} \left(\frac{V_N + V_S}{2} \right)^2 \quad (1)$$

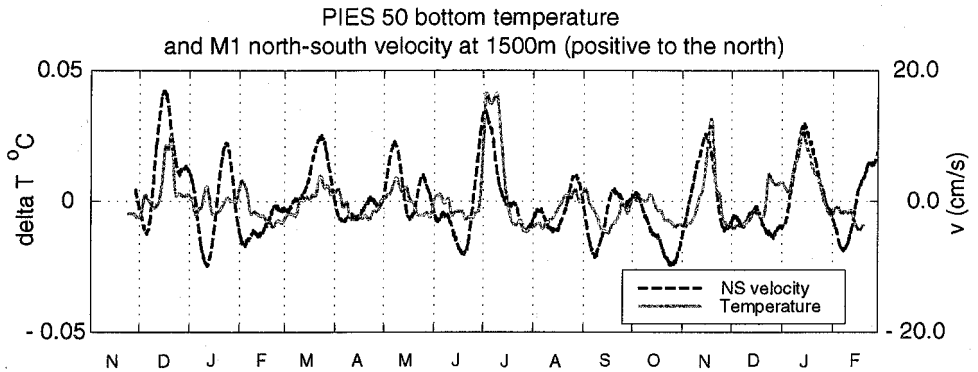


Figure 4. Time series of bottom temperature at PIES 50 and north-south velocity component of the M1 current meter at 1500 m.

and the conservation of mass

$$V_N A_N = V_S A_S \tag{2}$$

where λ is the coefficient of open channel hydraulic drag (Henderson, 1966), l is the distance between stations, d is the perimeter of a section, V is the mean velocity, and A is the cross section area. The subscript N is for the northern PIES location (PIES 62) and the subscript S is for the southern PIES location (PIES 50).

From Eqs. (1) and (2), for a given λ , it is possible to obtain V_N and V_S and from there to calculate the total transport $V_N A_N$ or $V_S A_S$. With only two instruments along the channel, the value of λ will have to be determined independently.

The transport obtained from the difference in pressure using the previous formulation is shown in (Fig. 5). The values of the parameters used are: $\rho_0 = 1025 \text{ kg/m}^3$, $l = 1.08 \times 10^5 \text{ m}$,

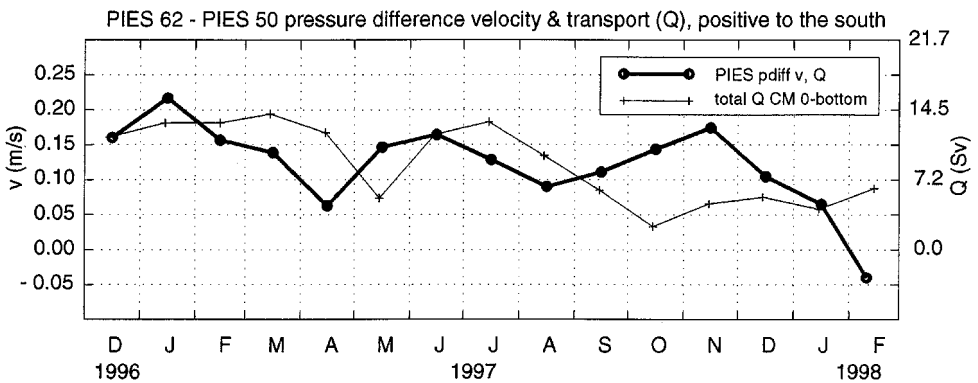


Figure 5. Velocity and transport obtained from pressure difference between PIES 62 and PIES 50 (positive to the South). Also shown is the total transport from CMM measurements (Gordon and Susanto, 1999).

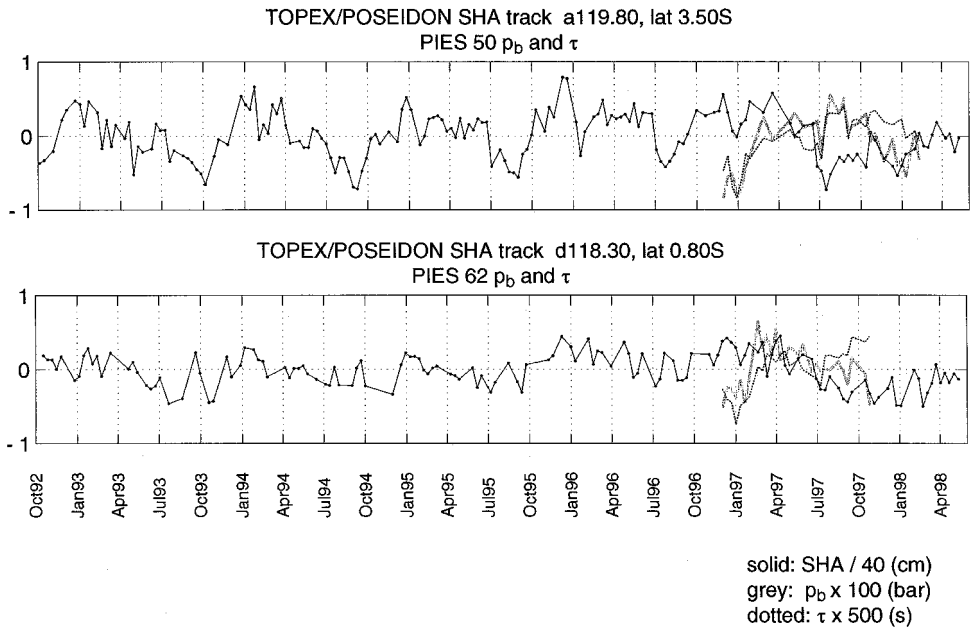


Figure 6. Time series of η' from T/P and τ and p_b from PIES.

$d = 4 \times 10^4$ m, $A_2 = 7.23 \times 10^7$ m², and $A_N/A_S = 3$. For comparison, it is superimposed to the transport measured with the CMM. It must be noted that the CMM transport is measured from 200 m to 1500 m. Values for the upper 200 m are extrapolated (Gordon and Susanto, 1999).

There is an apparent common trend to these two curves suggesting a possible low-frequency relationship that may be barotropic or involve two-layer behavior. The shorter term oscillations are not well correlated. Overall, however, the two-layer model fails to fit the observed currents and only achieves a correlation coefficient of 0.04. The shape of the curves is different and the value of λ , needed to obtain values of transport of the same order of magnitude, is too high ($\lambda = 2$). Typical values for λ are 0.1 or lower (Henderson, 1966). These results suggest that the bulk of the flow in the Makassar Strait is not driven by its barotropic pressure gradients. Based on these results, higher vertical resolution models will be tested for the Strait.

b. Altimetry data and the vertical structure of pressure gradient

Shown on Figure 6 are five years of time series of sea height anomaly η' from T/P track d118.30 at latitude 0.8S and track a119.80 at latitude 3.5S (Fig. 1). Superimposed on them are the τ and p_b time series from PIES 50 and PIES 62.

To a first approximation, many ocean areas can be modeled by a two-layer system. In a reduced gravity model, η' is linearly dependent on the depth of the thermocline h_1 (Goni et al., 1996).

$$\eta' = \varepsilon h_1 + B. \quad (3)$$

This relationship does not apply in the Makassar Strait. Direct comparisons between η' and τ in the Makassar Strait show little or no correlation for the period of measurement. This was also hinted at by the lack of correlation between τ and the depth of the upper thermocline (Fig. 2). However, there are some indications that, in the longer time scale (period of 200 days or more), η' is negatively correlated with τ , and with p_b . From November 1996 to October 1997 the sea height decreases. The positive sea height anomaly that normally starts in October (annual signal) does not appear in 1997 due to the shift of warm pool mass to the eastern Pacific during the strong El Niño year of 1997. The decrease in η' is accompanied by the increase in τ and p_b , and can be interpreted as dynamic height decrease caused by the presence of a layer colder than normal in the water column. Increases in τ and p_b are also results of this increase in the amount of the colder water.

The higher frequency fluctuation of η' (period shorter than 200 days) is less consistent with the change in τ and p_b . During some events, η' signal is in-phase with τ and p_b (for example the decrease in early January 1997). Other events show an out-of-phase relation between the η' and τ and p_b . This inconsistency reinforces the conclusion that the structure in the Makassar Strait involves dynamics more complicated than a simple two-layer system. In what follows, a three-layer model will be developed and applied to the Strait.

c. Makassar Strait dynamics in a three-layers approximation

A simple three-layer model is developed to study the time evolution at the two PIES locations. The water column is divided into three layers with mean thicknesses $h_1 = 200$ m, $h_2 = 300$ m, $h_3 = 1600$ m, densities $\rho_1 = 1022.97$ kg/m³, $\rho_2 = 1026.48$ kg/m³, $\rho_3 = 1027.40$ kg/m³, and sound speeds $c_1 = 1540.2$ m/s, $c_2 = 1519.4$ m/s and $c_3 = 1497.1$ m/s (Fig. 7). The densities and sound speeds are calculated from CTD profiles for the mean layer thickness chosen. The η' are from T/P track d118.30 at latitude 1.5S and track a119.80 at latitude 3.5S (Fig. 1).

Variations in layer thickness generate changes in p_b , τ , and η' . Three equations for changes in layer thickness can be constructed and solved using the observed η' , p_b , and τ .

$$\eta = -H + h_3 + h_2 + h_1 \quad (4a)$$

$$p_b = \rho_3 g h_3 + \rho_2 g h_2 + \rho_1 g h_1 \quad (4b)$$

$$\frac{1}{2} \tau = \frac{h_3}{c_3} + \frac{h_2}{c_2} + \frac{h_1}{c_1} \quad (4c)$$

$$\eta' = h'_3 + h'_2 + h'_1 \quad (5a)$$

$$p'_b = \rho_3 g h'_3 + \rho_2 g h'_2 + \rho_1 g h'_1 \quad (5b)$$

$$\frac{1}{2} \tau' = \frac{h'_3}{c_3} + \frac{h'_2}{c_2} + \frac{h'_1}{c_1}. \quad (5c)$$

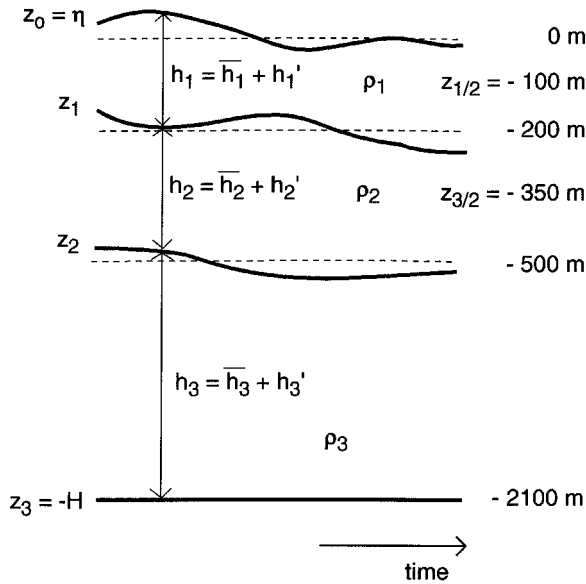


Figure 7. Schematic diagram of the three-layer model.

The primes indicate the deviation of the variables from their time mean. Figure 8a shows the solutions for the layer thickness changes at PIES 50 and PIES 60 locations.

Flow in a hydraulic controlled channel is subjected to the Bernoulli principle or energy conservation equation. In a nonfriction case, the energy exerted by pressure, potential energy and kinetic energy is constant.

$$\frac{D}{Dt} \left(\frac{p}{\rho} + \frac{v^2}{2} \right) = 0. \tag{6}$$

Assuming a constant potential energy, the change in kinetic energy between two locations in the channel can be related to the change in pressure.

$$\frac{D}{Dt} \left(\frac{p}{\rho} + \frac{v^2}{2} \right) = 0 \tag{7}$$

$$v_S^2 - v_N^2 = \frac{2}{\rho} (p_N - p_S). \tag{8}$$

Pressures in the middle of layer one and two (Fig. 8b) are calculated from layer thickness solutions.

$$p_1 = \rho_1 g (h_1 + h_2 + h_3 - H - z_{1/2}) \tag{9}$$

$$p_2 = \rho_1 g h_1 + \rho_2 g (h_2 + h_3 - H - z_{3/2}). \tag{10}$$

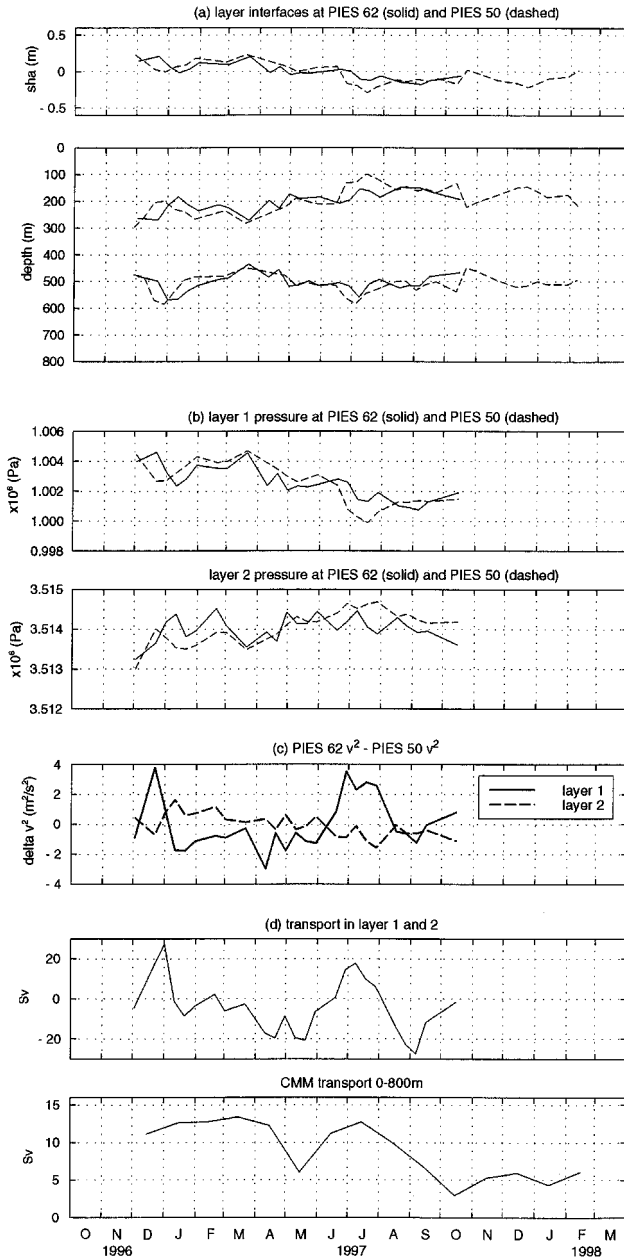


Figure 8. Results from the three-layer model: (a) layer interface change at PIES 62 and PIES 50. (b) pressure in the middle of layer 1 and 2. (c) kinetic energy change between PIES 62 and PIES 50. (d) transport in layer 1 and 2 (positive to the South). Also show is 0–800 m transport from CMM (Gordon and Susanto, 1999).

The kinetic energy change between PIES 62 and PIES 50 for the top two layers are calculated and shown in Figure 8c.

Using (8) and continuity (2), the absolute velocities in each layer can be determined.

$$v_s^2 = \frac{2r_A^2}{(r_A^2 - 1)\rho} (p_N - p_S) \quad (11)$$

where $r_A = A_N/A_S$.

Figure 8d shows the variability of the integrated transport in the two upper layers. Note that only variability is presented because there is an unknown mean pressure difference between the north and south location in the Bernoulli equation. The total transport will be the variability plus an added constant. Transport variability curves for each layer are directly proportional and are, therefore, not shown in Figure 8c.

4. Results

The model solutions for the three-layer system show some interesting results. (1) The top interface shoals (the top layer thickness decreases) during 1997. This is consistent with the strong El Niño onset in 1997 when the warm pool in the western equatorial Pacific moves eastward causing the thermocline to shoal in the Indonesian Seas. (2) The middle layer stretches in the opposite phase as compared with the top layer. The middle layer thickens during most of 1997. (3) The bottom layer has only slight changes during the measurement period. (4) A warm event, shown as a thickening of the middle layer, is observed first in the Labani constriction (PIES 50) around December 1996 and later on to the north (PIES 60) in January 1997.

The solutions for the thermal structure in the Makassar Strait depend mainly on the changes in the η' and the τ' . The changes in the p_b play a lesser role. The bottom pressure variability affects the mid-layer pressure and the transport variability calculation. This indicates that the thermal and flow structures in the Makassar Strait have a large baroclinic component.

Comparison between the model transport and the CMM (Fig. 8d) denotes that even though both curves follow a similar trend, the model variability is much larger. The correlation coefficient between the model combined (layer 1 and layer 2) transport and the observed transport is 0.36. The correlation coefficient for layer 2 and the observed transport is significantly larger at 0.64. Considering that conservation of energy is assumed when the velocities are derived, the model transport variability must be considered as the upper limit value. Energy loss due to friction and transfer to eddy kinetic energy should decrease the velocities. Comparison between the model derived and observed transport suggests that a significant amount of energy is lost in the process. The relatively small variability in the CMM transport can also be attributed to the fact that the CMM transport is extrapolated from 200 m up due to the lost upper-layer current meter. The model velocities suggest that most of the variability is in the top layer and the CMM values basically missed the entire top layer.

5. Summary and conclusions

It was widely assumed that the main throughflow in the Makassar Strait could be obtained in a first approximation by the differences between the pressure along the Strait. While the results presented are not conclusive due to the loss of the southernmost instrument, the results from the present study reveal new aspects about the highly baroclinic structure of the flow along the Makassar Strait. The combined measurements of surface height, integrated thermal structure and bottom pressure show that the vertical nature of the throughflow requires at least a three-layer description. The layer structure chosen here fits the data used in this study and is consistent with water mass structures observed. In the upper 200 m (the upper layer in the model) the water mass in the Makassar Strait is characterized by the salinity maximum of the North Pacific Subtropical Water. The water in layer 2 is characterized by the North Pacific Intermediate Water salinity minimum (Hautala *et al.*, 1996; Waworuntu *et al.*, 2000). The resolution of the present analysis cannot provide any more detail than the three-layer description. The contribution of the three data types used here does supply an assessment of the contributions of different layers. The conclusion is that the upper layer has the highest kinetic energy associated with large change in thickness. The thicker second layer is as important, however, in terms of transports. Priorities for future observations are larger-scale pressure measurements of the type described here and surface current observations.

Acknowledgments. This research was funded by ONR grants N00014-96-1-0831, N00014-99-F-0001 and JPL/NASA 960606. The T/P SHA data were provided by Dr. R. Cheney, NOAA Lab for Satellite Altimetry, Silver Spring, MD. Gratitude is extended to Drs. Indroyono Soesilo and Basri M. Gani of BPPT and Dr. Arnold Gordon of LDEO for leading and co-ordinating the ARLINDO project; Debbie Willey for computer support; Mike Rebozo and Robert Jones for the PIES deployment and recovery; Andreas Roubicek for the data reduction process; Roberta Lusic for preparing the manuscript for publication and to Captain Handoko and the crew of KAL *Baruna Jaya IV*.

REFERENCES

- Bingham, F. M. and R. Lukas. 1995. The distribution of intermediate water in the western equatorial Pacific during January–February 1986. *Deep-Sea Res.*, *42*, 1545–1573.
- Ffield, A. and A. L. Gordon. 1992. Vertical mixing in the Indonesian thermocline. *J. Phys. Oceanogr.*, *22*, 184–195.
- Garzoli, S. L. 1993. Geostrophic velocity and transport variability in the Brazil-Malvinas Confluence. *Deep-Sea Res.*, *40*, 1379–1403.
- Garzoli, S. L. and Z. Garraffo. 1989. Transports, frontal motions and eddies at the Brazil-Malvinas Currents Confluence. *Deep-Sea Res.*, *36*, 681–703.
- Garzoli, S. L., G. Goni, A. J. Mariano and D. B. Olson. 1997. Monitoring the upper southeastern Atlantic transport using altimeter data. *J. Mar. Res.*, *55*, 453–481.
- Garzoli, S. L., A. L. Gordon, V. Kamenkovich, D. Pillsbury and C. Duncombe-Rae. 1996. Variability and sources of the southeastern Atlantic circulation. *J. Mar. Res.*, *54*, 1039–1071.
- Goni, G., S. Kamholz, S. L. Garzoli and D. B. Olson. 1996. Dynamics of the Brazil-Malvinas Confluence based on inverted echo sounders and altimetry. *J. Geophys. Res.*, *101*, 16273–16289.

- Gordon, A. L. and R. A. Fine. 1996. Pathways of water between the Pacific and Indian oceans in the Indonesian seas. *Nature*, 379, 146–149.
- Gordon, A. L. and R. D. Susanto. 1999. Makassar Strait transport: Initial estimate based on Arlindo results. *Mar. Tech. Soc.*, 32, 34–45.
- Gordon, A. L., R. D. Susanto and A. Ffield. 1999. Throughflow within Makassar Strait. *Geophys. Res. Lett.*, 26, 3325–3328.
- Gordon, A. L., R. D. Susanto, A. Ffield and D. Pillsbury. 1998. Makassar Strait Transport: Preliminary Arlindo results from MAK-1 and MAK-2. *WOCE Intl. Newsletter*, 33, 30–32.
- Hautala, S. L., J. L. Reid and N. Bray. 1996. The distribution and mixing of Pacific water masses in the Indonesian Seas. *J. Geophys. Res.*, 101, 12375–12389.
- Henderson, F. M. 1966. *Open Channel Flow*, Macmillan series in civil engineering, Macmillan, 522 pp.
- Ilahude, A. G. and A. L. Gordon. 1996. Thermocline stratification within the Indonesian Seas. *J. Geophys. Res.*, 101, 12401–12409.
- Katz, E. J. 1977. Zonal pressure gradient along the equatorial Atlantic. *J. Mar. Res.*, 35, 293–307.
- Kelly, K. A. and D. R. Watts. 1994. Monitoring Gulf Stream transport by radar altimetry and inverted echo sounders. *J. Phys. Oceanogr.*, 24, 1080–1084.
- Watts, D. R. and T. Rossby. 1977. Measuring dynamic heights with inverted echo sounders: Results from MODE. *J. Phys. Oceanogr.*, 7, 345–358.
- Waworuntu, J. M., R. A. Fine, D. B. Olson and A. L. Gordon. 1999. Spreading and velocity patterns of the Indonesian Throughflow. *Intl. WOCE Newsletter*, 35, 26–28.
- 2000. Recipe for the Banda Sea Water. *J. Mar. Res.*, 58, 547–569.